Supporting Information

Chung et al. 10.1073/pnas.1220603110

SI Materials and Methods

Generation of Lung-Specific *Mammalian Sterile 20-Like Kinase 1/2*-Knockout Mice and Genotyping. The generation of *mammalian sterile 20-like kinase-2* (*Mst2*)-null mice in a C57BL/6 background has been previously described (1). *Mst1*$^{fl/fl}$ mice were kindly provided by T.K. and have been previously described (2). *Nkx2.1*-Cre transgenic mice were obtained from Jackson Laboratories and have been previously described (3). *Mst1*$^{fl/fl}$; *Mst2*-null mice, generated by crossing *Mst1*$^{fl/fl}$ and *Mst2*-null mice were bred with *Nkx2.1*-Cre mice to generate *Mst1*$^{fl/fl}$;*Mst2*$^{-/-}$;*Nkx2.1*-Cre mice. *Mst2*$^{-/-}$ mice showed no lung abnormalities, as previously reported (4). WT mice or *Mst2*$^{-/-}$ mice were used as controls. Recombination of *Mst1* was confirmed by PCR analysis. Primers for recombination analysis were 5′-AGG GAC CAA GGA CCC TGC AGG-3′, 5′-TGG GGG TGT GCC AGG TCC AA-3′, and 5′-GCG AAT TCT TAA GCC TGG CGC TTC-3′.

Histological Analysis. Antibodies for immunostaining included those to surfactant protein-B (SP-B), CC10, and TAZ (transcriptional coactivator with PDZ-binding motif) (Santa Cruz Biotechnology); YAP (Yes-associated protein), Ser^{127}-phosphorylated YAP, and Foxa2 (forkhead box A2) (Cell Signaling); acetylated tubulin and α-SMA (smooth muscle actin) (Sigma); TTF-1 (thyroid transcription factor-1) and platelet endothelial cell adhesion molecule (PECAM) (Dako); pro–SP-C (Millipore); T1α (clone 8.1.1; University of Iowa Hybridoma Bank); Sox9 (sex-determining region Y box 9, a marker for distal lung progenitor cells) (Santa Cruz Biotechnology); Sox2 (Cell Signaling); and BrdU (BD Biosciences).

Immunoblot Analysis. Antibodies for immunoblotting included those to YAP, Ser^{127}-phosphorylated YAP, WW45, MST1, Mst2, and large tumor suppressor 1 (LATS1) (Cell Signaling); LATS2 (Bethyl Laboratories); β-actin (Sigma); CTGF (connective growth tissue factor) (Santa Cruz Biotechnology); Foxa2 (Cell Signaling); and GAPDH (Abcam).

Dry Lung Weight. The dry lung weight was determined as described previously (5) with some modification. Mice were killed and both lungs were excised. Lungs were then dried to constant weight in a microwave oven for 60 min and were weighed.

Retrovirus Preparation and Infection. For preparation of retroviral particles, 293T cells were transfected with pMSCV vectors encoding HA- or Flag-tagged Mst1 or empty vector using polyethyleneimine. After 3 d, the medium containing retrovirus was harvested and passed through a 0.2-μm pore diameter syringe filter. A549 or MLE-12 cells were infected with retrovirus for 6 h using polybrene (8 μg/mL).

Lentiviral Transduction. Cell lines stably expressing Mst1 and Mst2 shRNA were established using a vector-based shRNA technique. The mouse Mst1 and Mst2 shRNA targets were 5′-CCG TCT TTC CTT GAA TAC TTT-3′ and 5′-CCC ATG ATG GAA CGA GAA ATA-3′, respectively. The human Mst1 and Mst2 shRNA targets were 5′- GGG CAC TGT CCG AGT AGC AGC -3′ and 5′- CCG GTC AAG TTG TCG CAA TTA -3′, respectively. The shRNA control (scrambled) sequence was 5′-CGT ACG CGG AAT ACT TCG ATT-3′. Lentiviruses were produced by cotransfecting subconfluent 293T cells with an expression plasmid (pLKO.1) and packing plasmids (psPAX2 and pMD 2G) using polyethyleneimine. Murine lung epithelial (MLE)-12 cells were infected with the lentivirus containing Mst1 and Mst2 or scrambled nontarget shRNA. Mst1 and Mst2 knockdown efficiency was determined by Western blotting. Mouse YAP and TAZ SiRNA target sequences were 5′-CGG TTG AAA CAA CAG GAA TTA-3′ and 5′- CCA TGA GCA CAG ATA TGA GAT-3′, respectively.

In Vitro Kinase Assay. The protocol and methods for in vitro kinase assays were as described previously (6), with some modifications. In vitro kinase assays with WT Mst1-Flag or kinase-dead (KD) Mst1-Flag, a fusion protein of GST and the forkhead domain of Foxa2 was used as a substrate. WT Mst1-Flag and KD Mst1-Flag were precipitated with an anti-Flag antibody. Mst1 kinase activity was measured by incubating substrate and kinase in kinase buffer [40 mM Hepes, 20 mM $MgCl_2$, 1 mM DTT, 0.1 mM Na_3VO_4, and 3 μCi (γ^{32}-P) ATP] for 30 min at 30 °C. The level of phosphorylated Foxa2 was measured by autoradiography.

In vitro kinase assays with LATS2 was performed similarly with cell lysates containing WT Lats2-HA or KD Lats2-HA and Mob1-Flag immunoprecipitated with anti-HA antibody.

BrdU Labeling. BrdU labeling and detection were performed as described by Lee et al. (7). Briefly, pregnant females were injected intraperitoneally with BrdU (Sigma) at a concentration of 100 μg/g body weight and killed 1 h later for each embryonic day. Embryos were processed for immunostaining with antibody against BrdU for counting and quantification under fluorescence microscopy.

Transmission Electron Microscopy. Electron microscopy analyses of lung and cell samples were performed according to standard protocols as previously described (7). The samples were fixed with 3% glutaraldehyde in PBS for 2 h, then washed with 0.1 M cacodylate buffer (pH 7.2) containing 0.1% $CaCl_2$ at 4 °C. Samples were postfixed with 1% OsO_4 in 0.1 M cacodylate buffer and dehydrated with an ethanol series and propylene oxide. The samples were embedded in Embed-812 (Electron Microscopy Sciences), cut with a diamond knife on an ULTRACUT UC7 μLtramicrotome (Leica), and mounted on Formvar-coated slot grids. Sections were stained with 4% uranyl acetate and lead citrate and observed using an H-7650 transmission electron microscope (Hitachi).

Scanning Electron Microscopy. The samples were fixed in a 2.5% paraformaldehyde-glutaraldehyde mixture buffered with 0.1 M phosphate (pH 7.2) for 2 h, postfixed in 1% OsO_4 in the same buffer for 1 h, dehydrated in graded ethanol, and substituted with isoamyl acetate. After drying at the critical point in CO_2, samples were sputtered with gold in a sputter coater (SC502; Polaron) and observed using an S4300N scanning electron microscope (Hitachi) installed at the Korea Research Institute of Bioscience and Biotechnology.

1. Oh S, et al. (2009) Crucial role for Mst1 and Mst2 kinases in early embryonic development of the mouse. *Mol Cell Biol* 29(23):6309–6320.
2. Katagiri K, et al. (2009) Mst1 controls lymphocyte trafficking and interstitial motility within lymph nodes. *EMBO J* 28(9):1319–1331.
3. Tiozzo C, et al. (2009) Deletion of Pten expands lung epithelial progenitor pools and confers resistance to airway injury. *Am J Respir Crit Care Med* 180(8):701–712.
4. Zhou D, et al. (2009) Mst1 and Mst2 maintain hepatocyte quiescence and suppress hepatocellular carcinoma development through inactivation of the Yap1 oncogene. *Cancer Cell* 16(5):425–438.
5. Petersen B, et al. (2007) Activation of Toll-like receptor 2 impairs hypoxic pulmonary vasoconstriction in mice. *Am J Physiol Lung Cell Mol Physiol* 94(2):300–308.
6. Song H, et al. (2012) Ablation of Rassf2 induces bone defects and subsequent haematopoietic anomalies in mice. *EMBO J* 31(5):1147–1159.
7. Lee JH, et al. (2008) A crucial role of WW45 in developing epithelial tissues in the mouse. *EMBO J* 27(8):1231–1242.

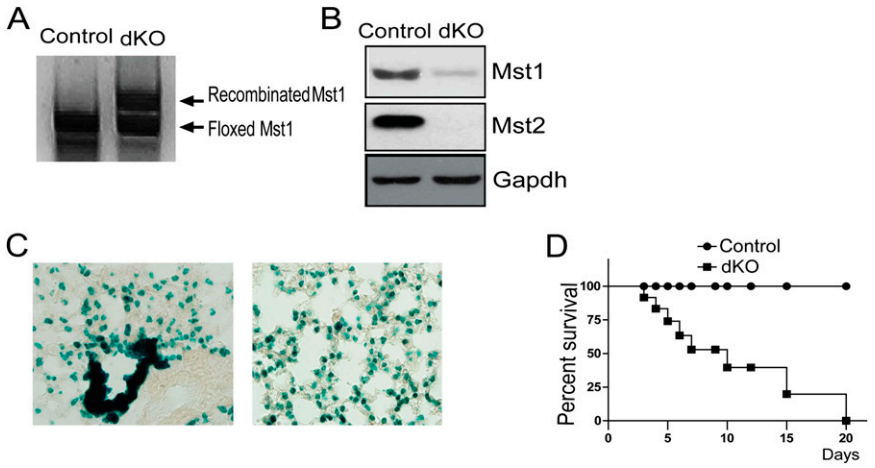

Fig. S1. Generation of lung-specific *Mst1* and *Mst2* knockout mice. (*A*) Recombination PCR analysis of lung tissue from *Mst1/2*-double-knockout (dKO) mice. (*B*) Lung homogenates from *Mst1/2*-dKO mice and control mice were analyzed by immunoblotting using antibodies to Mst1 and Mst2. (*C*) Detection of Cre-induced β-galactosidase in the lungs of Rosa26R$^{nkx2.1\text{-}cre}$ mice at PN1. Lac-Z expression was detected in type II pneumocytes, with the strongest staining observed at the airway level. (Magnification: 200×.) (*D*) Kaplan-Meier survival curves from control and *Mst1/2*-dKO mice (n = 10 each); the median survival of the latter was 10 d (P = 0.0061).

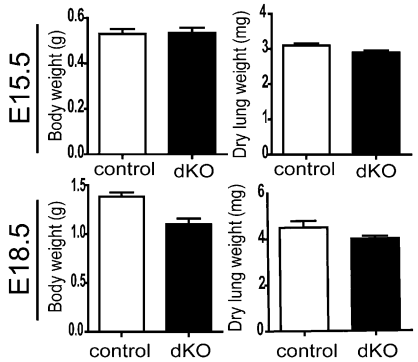

Fig. S2. Evaluation of embryonic lung size and dry lung weight. Quantification of body weight and dry lung weight of control and *Mst1/2*-dKO mice at embryonic day (E)15.5 and E18.5. Body weight and dry lung weight were comparable between control and *Mst1/2*-dKO mice at E15.5 and E18.5. Pictures of representative lungs are shown in Fig. 1*A*.

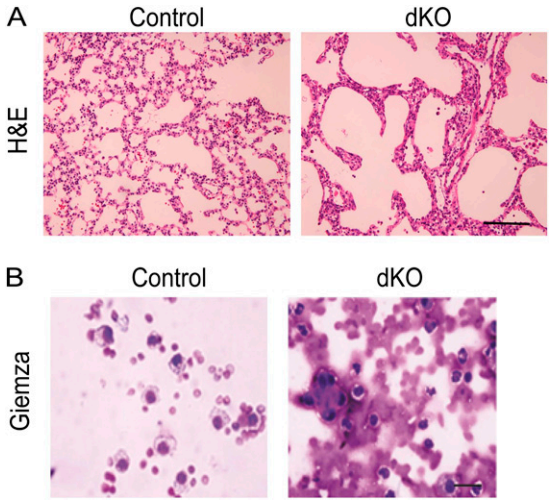

Fig. S3. Emphysematous lesion and analysis of bronchoalveolar lavage (BAL) fluid in postnatal day (PN)10 *Mst1/2* dKO mice. (*A*) Lung section from PN10 control and *Mst1/2*-dKO mice were stained with H&E, revealing emphysematous lesion in *Mst1/2*-dKO mice. (Scale bar, 200 μm.) (*B*) BAL cytology was determined at PN10. Briefly, mice were anesthetized with pentobarbital sodium (60 mg/kg; Hanlim Pharma) and intubated using a 20-gauge cannula. After intubation, BAL cells were collected by lavaging whole lungs with 1 mL PBS via the tracheal cannula by withdrawing slowly while gently massaging the thorax. Cells (1–5 × 10^3 cells) were spun onto glass slides (Cytospin 2; Shandon Instruments), air dried, fixed with methanol, and stained using the Hema 3 system (Thermo Fisher Scientific). There were numerous RBCs and lymphocytes in *Mst1/2*-dKO mice BAL, but no bacteria or fungi were found, thereby ruling out infection. (Scale bar, 20 μm.)

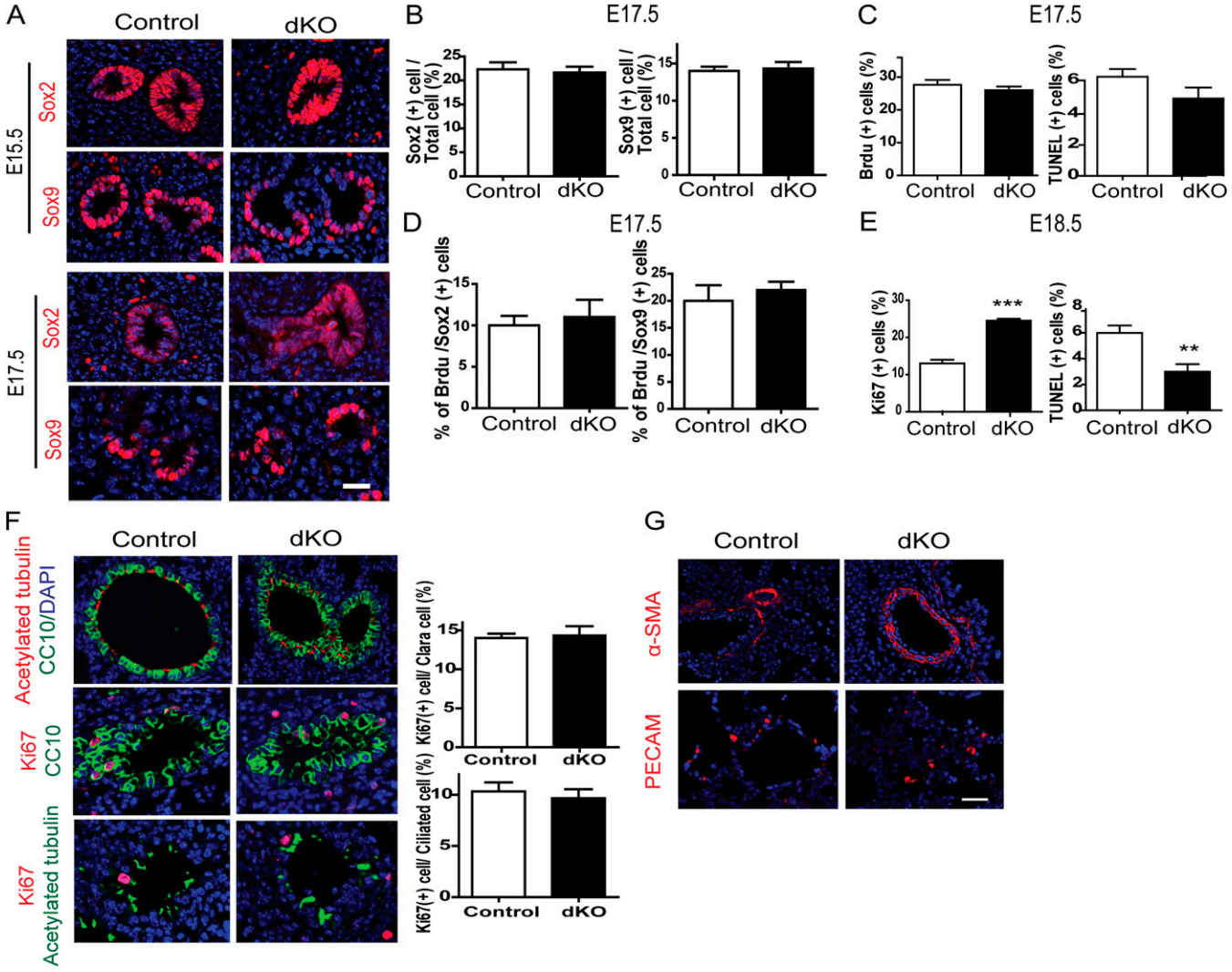

Fig. S4. Expression of epithelial progenitor markers and proliferation of airway epithelial cells. (*A*) Immunostaining shows similar expression levels of Sox2 (proximal epithelial progenitor marker) and Sox9 (distal epithelial progenitor marker) at E15.5 and E17.5. (Scale bar, 50 μm.) (*B*) Quantification of distal and proximal epithelial progenitor cells at E17.5. (*C*) Quantification of Brdu (+) cell and TUNEL (+) cell at E17.5. Representative pictures are in Fig. 1*D*. (*D*) BrdU labeling of distal and proximal progenitor at E17.5 were determined as percentage of $Sox2^+$,$Brdu^+$ or $Sox9^+$,$Brdu^+$ cells after 1-h pulse labeling (Scale bar, 50 μm). Representative pictures are in Fig. 1*D*. (*E*) Quantification of Ki67 (+) and TUNEL (+) cells at E18.5. Representative pictures are Fig. 1*E*. $^{**}P < 0.01$, $^{***}P < 0.001$. (*F*) E18.5 mice lungs were stained with antibodies to acetylated tubulin, CC10, and Ki67 to check their distribution and proliferation of ciliated cell and Clara cell. Quantification of Ki67 (+) cells among Clara cells or ciliated cells showed that the proliferation of the airway epithelial cells was similar between *Mst1/2* dKO and control mice. Magnification: 400×. (*G*) E18.5 mice lungs were stained with antibodies to α-SMA (smooth muscle cells), and PECAM (vascularity). α-SMA staining, a marker for bronchial smooth muscle and pulmonary arteries, was similar in control and *Mst1/2*-dKO mice. There were no alterations in smooth muscle cells and vascular network between control and *Mst1/2*-dKO mice. (Scale bar, 20 μm.)

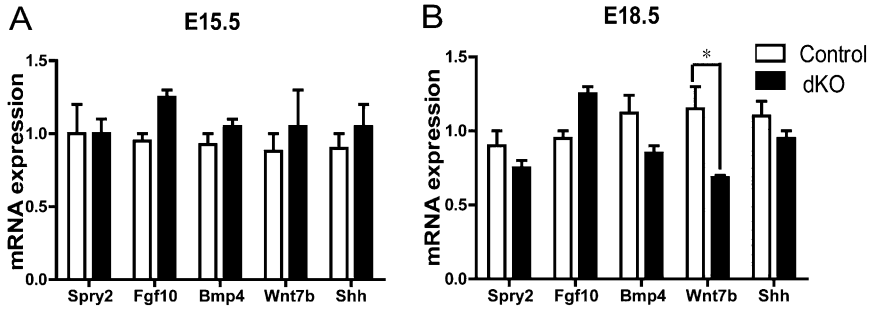

Fig. S5. Expression of cardinal signaling of branching morphogenesis. (*A* and *B*) Quantitative RT-PCR analyses of the mRNA expression of cardinal signaling genes during lung morphogenesis at E15.5 and E18.5. The expressions of Sprouty homolog-2 (Spry2), fibroblast growth factor (Fgf)10, bone morphogenetic protein 4 (Bmp4), and Sonic Hedgehog (Shh) were similar between control and *Mst1/2*-dKO mice. Wnt7b was decreased in *Mst1/2*-dKO mice at E18.5.

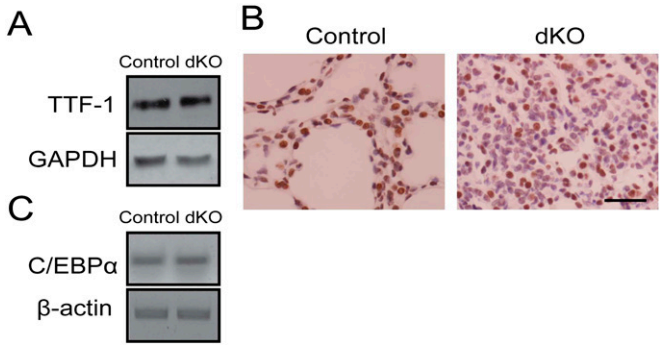

Fig. S6. Expression of TTF-1 and C/EBPα (CCAAT/enhancer binding protein-α). (*A* and *B*) Western blotting and immunohistochemistry demonstrate that expression of TTF-1 was not altered in *Mst1/2*-dKO mice. Lung homogenates and lung sections were prepared form E18.5 mice. (Scale bar, 50 μm.) (*C*) C/EBPα mRNA was similar in control and *Mst1/2*-dKO mice. Total lung RNA was prepared from E18.5 mice.

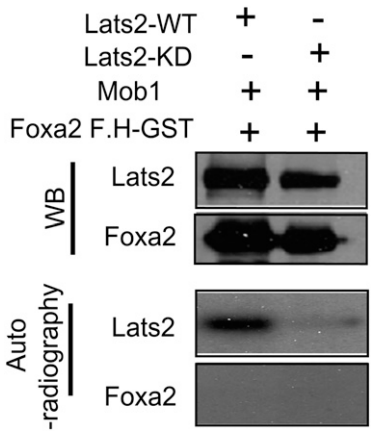

Fig. S7. Lats2 does not phosphorylate the forkhead domain of Foxa2. In vitro kinase assay. Anti-HA immunoprecipitates prepared from 293T cell lysates expressing HA-tagged WT or Kinase-dead (KD) Lats2 and Flag-tagged Mob1 were assayed for kinase activity. GST fused with the forkhead domain of Foxa2 was used as a substrate. After autoradiography, the membrane was blotted with anti-Lats2 Antibody and anti-Foxa2 antibody to reveal substrate input. Autoradiography showed that WT Lats2 was autophosphorylated as predicted, but forkhead domain of Foxa2 was not phosphorylated.

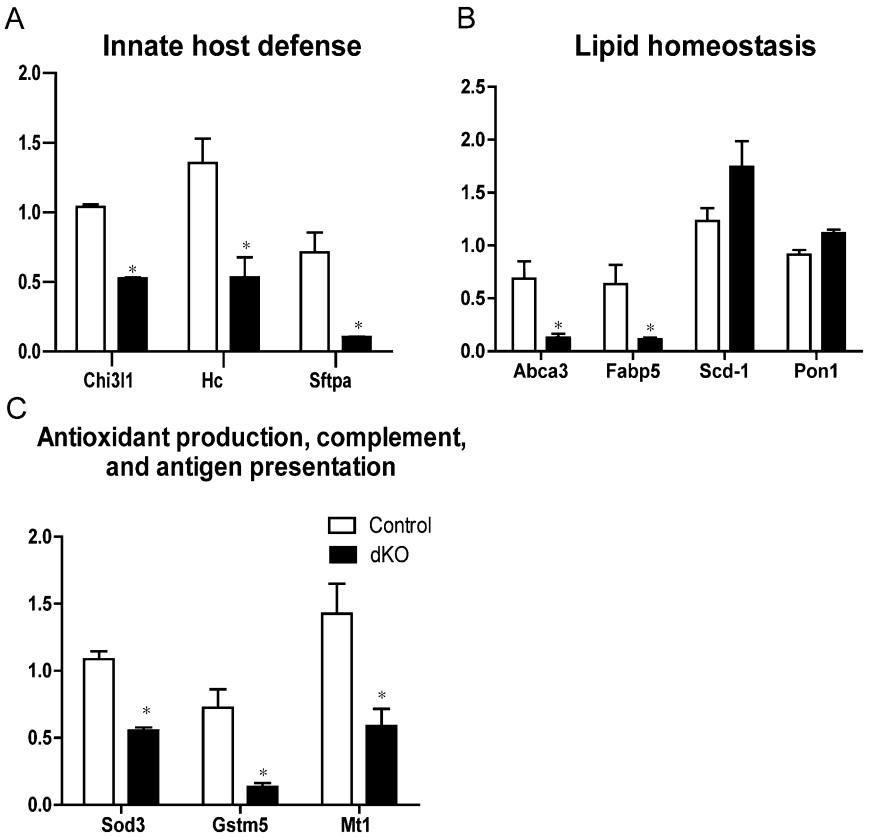

Fig. S8. Characterization of Foxa2 contribution in the *Mst1/2*-dKO mice phenotype. Quantitative RT-PCR analyses of the representative Foxa2 target genes involved in (*A*) innate host defense (Chil3l1, Hc, and Sftpa), (*B*) lipid homeostasis (Abca3, Fabp5, Scd-1, and Pon1), and (*C*) antioxidant production(Sod3, Gstm5, and Mt1) found by Whitsett and colleagues (1) in *Mst1/2* dKO mice. $*P < 0.05$.

1. Wan H, et al. (2004) Foxa2 is required for transition to air breathing at birth. *Proc Natl Acad Sci USA* 101(40):14449–14454.

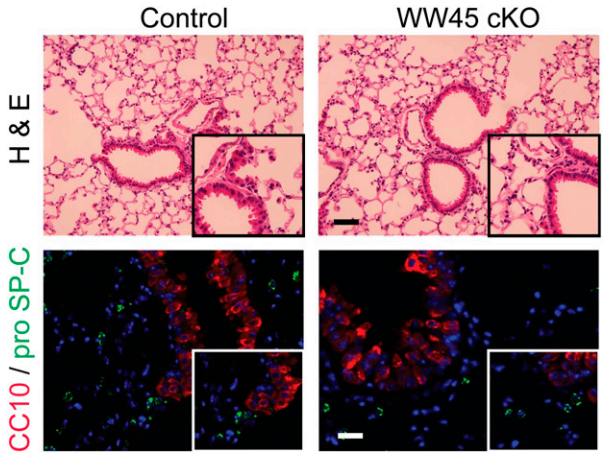

Fig. S9. Deletion of mammalian Salvador (*WW45*) causes no abnormalities in lung during development. Lung sections from control and *WW45*-cKO (*WW45*$^{f/f}$; *Nkx2.1*-Cre) mice at 3 mo were stained with H&E. *WW45*-cKO mice were born normally and showed no developmental defects or other abnormalities. (Scale bar, 50 μm.) Immunofluorescence analyses showed no alterations in CC10 or proSP-C in *WW45*-cKO mice. (Scale bar, 25 μm.)

Table S1. Summary of comparison between Foxa2 KO and *Mst1/2* dKO lung transcriptomes

Category	Genes	Foxa2 KO	Mst1/2 dKO
Innate host defense	*Chi3l1*	▼	▼
	Hc	▼	▼
	Sftpa	▼	▼
Lipid homeostasis	*Abca3*	▼	▼
	Fabp5	▼	▼
	Scd-1	▼	—
	Pon1	▼	—
Antioxidant production	*Sod3*	▲	▼
	Gstm5	▲	▼
	Mt1	▲	▼

Published microarray data of Foxa2 KO mice showed significant decrease of genes related to innate host defense (*Chi3l1*, *Hc*, and *Sftpa*) and lipid homeostasis (*Abca3*, *Fabp5*, *Scd1*, and *Pon1*). Genes regulating antioxidant production (*Sod3*, *Gstm5*, and *Mt1*) were increased in Foxa2 KO mice. The quantitative RT-PCR results showed that, like *Foxa2*-null mice, *Mst1/2* dKO mice have decreased expression of genes related to innate host defense, such as *Chi3l1* and *Hc* and genes regulating lipid homeostasis, including *Fabp5* and *Abca3*. Up triangle means that the gene expression of mutant mice is higher than that of control. Down triangle means that the gene expression of mutant mice is lower than that of control. Dashes indicate that gene expression of mutant and control is not significantly different.

Table S2. Primers for quantitative real-time PCR analysis

Gene	Forward primer (5′–3′)	Reverse primer (5′–3′)
SP-A	GAGGAGCTTCAGACTGCACTC	AGACTTTATCCCCCACTGACAG
SP-B	CTGCTTCCTACCCTCTGCTG	CTTGGCACAGGTCATTAGCTC
SP-C	ATGGACATGAGTAGCAAAGAGGT	CACGATGAGAAGGCGTTTGAG
SP-D	AAGGTCCACGGGGTGAGAA	TTTGCCTTGAGGTCCTATGTTC
T1α	ACCGTGCCAGTGTTGTTCTG	AGCACCTGTGGTTGTTATTTTGT
ABCA3	CAGCTCACCCTCCTACTCTG	ACTGGATCTTCAAGCGAAGCC
FOXA1	CCCTACGCCAACATGAACTCG	GTTCTGCCGGTAGAAAGGGA
FOXA2	ATGAGAGCAACGACTGGAACA	TCATGGAGTTCATAGAGCCCAC
C/EBPα	CAAGAACAGCAACGAGTACCG	GTCACTGGTCAACTCCAGCAC
TTF-1	AGGACACCATGCGGAACAG	CCATGCCGCTCATATTCATGC
YAP	TACTGATGCAGGTACTGCGG	TCAGGGATCTCAAAGGAGGAC
TAZ	CATGGCGGAAAAAGATCCTCC	GTCGGTCACGTCATAGGACTG

Table S3. Primers for cardinal signaling of lung morphogenesis related genes

Gene	Forward primer (5′–3′)	Reverse primer (5′–3′)
Spry2	TGTGAGGACTGTGGCAAGTGC	TTTAAGGCAACCCTTGCTGG
FGF10	GAGAAGAACGGCAAGGTCAG	GGAGGAAGTGAGCAGAGGTG
BMP4	AGGAGGAGGAGGAAGAGCAG	TGTGATGAGGTGTCCAGGAA
Wnt7b	CCCACATGACAGATGGACAG	GGACCCTGAAGCAGGTATCA
Shh	GAAGATCACAAGAAACTCCGAACG	TGGATTCATAGTAGACCCAGTCGAA

Table S4. Primers for Foxa2 target genes

Gene	Forward primer (5′–3′)	Reverse primer (5′–3′)
Scd1	TTCTTGCGATACACTCTGGTGC	CGGGATTGAATGTTCTTGTCGT
Pon1	AAGAACCATCGGTCTTCCTATCA	AGCACCCGTCTCGATTCCT
Fabp5	CATCACGGTCAAAACCGAGAG	ACTCCACGATCATCTTCCCAT
Hc	CAGCCCAATCAAGTTCCTAGAG	CGGCGTGTAAACAGGTTTGTC
Chi3l1	ATGCACACCTCTACTGAAGCC	ACCAGCTTGTACGCAGAGC
Mt1	AAGAGTGAGTTGGGACACCTT	CGAGACAATACAATGGCCTCC
Gstm5	AGAAACGGTACATCTGTGGGG	GGATGGCGTTACTCTGGGTG
Sod3	ACCGGCTTGGTTCTCTTCC	CTCCATCGGGTTGTAGTGCG
Foxj1	CCCTGACGACGTGGACTATG	GCCGACAGAGTGATCTTGGT